Supporting information

Directed self-assembly strategy of DET complex based on the application of artificial electron channeling

Zhan Song[1], Meijing Wei[1], Yinghao Fang[1], Fuping Lu[1], Minze Jia[b], Hui-Min Qin[1,*], and Shuhong Mao[1,*]

[1] *Key Laboratory of Industrial Fermentation Microbiology of the Ministry of Education; Tianjin Key Laboratory of Industrial Microbiology; College of Biotechnology, Tianjin University of Science and Technology; National Engineering Laboratory for Industrial Enzymes; Tianjin 300457, P. R. China*

*Corresponding authors: College of Biotechnology, Tianjin University of Science and Technology,

H.-M. Qin: huiminqin@tust.edu.cn;

S. Mao: shuhongmao@tust.edu.cn.

Tel: +86-22-60602949. Fax: +86-22-60602298

Contents

Table S1 Bacterial strains and plasmids used in this study

Strains and plasmids	Description	Source
Strains		
E. coli JM109	cloning	Lab stock
E. coli BL21 (DE3)	expression	Lab stock
KshA-BL21	pET28a carries *KshA*; BL21 (DE3)	Lab stock
PRF-BL21	pET28a carries reductase domain and ferredoxin of CYP116B46; BL21 (DE3)	Lab stock
DmFdx2-BL21	pET28a carries *DmFdx2* gene; BL21 (DE3)	Lab stock
FDH- BL21	pET28a carries *FDH* gene; BL21 (DE3)	Lab stock
Plasmids		
pET28a-KshA	pET28a, contain *KshA* gene (codon-optimized), KanR	Lab stock
pET28a-PRF	pET28a, contain *PRF* gene (codon-optimized), KanR	Lab stock
pET28a-DmFdx2	pET28a, contain *DmFdx2* gene (codon-optimized), KanR	Lab stock
pET28a- FDH	pET28a, contain *FDH* gene (codon-optimized), KanR	Lab stock
Mutant MT1	pET28a, contain Y110R in *KshA* gene, KanR	This study
Mutant MT2	pET28a, contain Y110R in *KshA* gene, T85D in *DmFdx2* gene, KanR	This study
Mutant MT3	pET28a, contain Y110R/Y226M in *KshA* gene, T85D in *DmFdx2* gene, KanR	This study

Table S2. Primers used in this study.

Mutations	Primmer	Template	Sequence (5' to 3')
Alanine scanning			
V259A	V259A-F	PRF	CAAGCGGTGCTGAGAAACAGTGGC
	V259A-R		AAATGGTCTTTCTTTGGCAGGATCCAGATG
Q260A	Q260A-F		TTTGCAGTGGTGCTGAGAAACAGTGG
	Q260A-R		ATCTCTATTCTCAGGATCACTACACAGGCT
			ATACTGTCTGC
S261A	S261A-F		AACGCTGGCCTGACTGTGGAAGTG
	S261A-R		TCTCAGCACCACTTGAAATGGTCTTTCTTTG
E264A	E264A-F		GTGGCAGTGCCTGCAGATAAAACCC
	E264A-R		GTCAGGCCACTGTTTCTCAGCACCAC
W97A	W97A-F	KshA	GATGCGCGTTGGGGTGGTAATG
	W97A-R		GTGGAATGGG CACGCGATGC
P109A	P109A-F		ATCGCGTATGCCCGTCGTGTTC
	P109A-R		CGCGGTGCACTTGCCATTACC
Y110A	Y110A-F		CCGGCTGCCCGTCGTGTTC
	Y110A-R		GATCGCGGTGCACTTGCCATTACC
R112A	R112A-F		CGTGCTGTTCCACCGCTGGC
	R112A-R		GGCATACGGGATCGCGGTGC
T85A	T85A-F	DmFdx2	CTGGCCTGCAGCACCTGCC
	T85A-R		AGTGCCTTCGCAGGCACCAAAG
T88A	T88A-F		AGCGCCTGCCACCTGATTTTTAAAAC
	T88A-R		GCAGGTCAGAGTGCCTTCGCAG
Site-saturation mutagenesis			
Y110	Y110-F	KshA	CCGNNNGCCCGTCGTGTTC
	Y110-R		CCGNNKGCCCGTCGTGTTCCAC
Y110R/W97	Y110R/W97-F	MT1	GATNNKCGTTGGGGTGGTAATGGC
	Y110R/W97-R		GTGGAATGGGCACGCGATGC
Y110R/Y226	Y110R/Y226-F	MT1	AATNNKGGTGATCCGAATGCGGTGC
	Y110R/Y226-R		CGTGCCACTGATGATATCTTCACGGC
T85	T85-F	PRF	CTGNNKTGCAGCACCTGCCACC
	T85-R		AGTGCCTTCGCAGGCACCAAAG

Table S3. Characteristics of the resins used in this study.

Name	Chemical composition	Pore size (μm)	Surface area (m^2/g)	Swelling in water
ES103B	Epoxy-polyacrylic ester	300-450	100-140	no
ES108	Epoxy-polyacrylic ester	300-450	100-140	no
ESQ3	Epoxy-polyacrylic ester	300-450	100-140	no
ER3	Epoxy-polyacrylic ester	300-450	80-120	no
ER8	Epoxy-polyacrylic ester	300-450	80-120	no

Figure S1

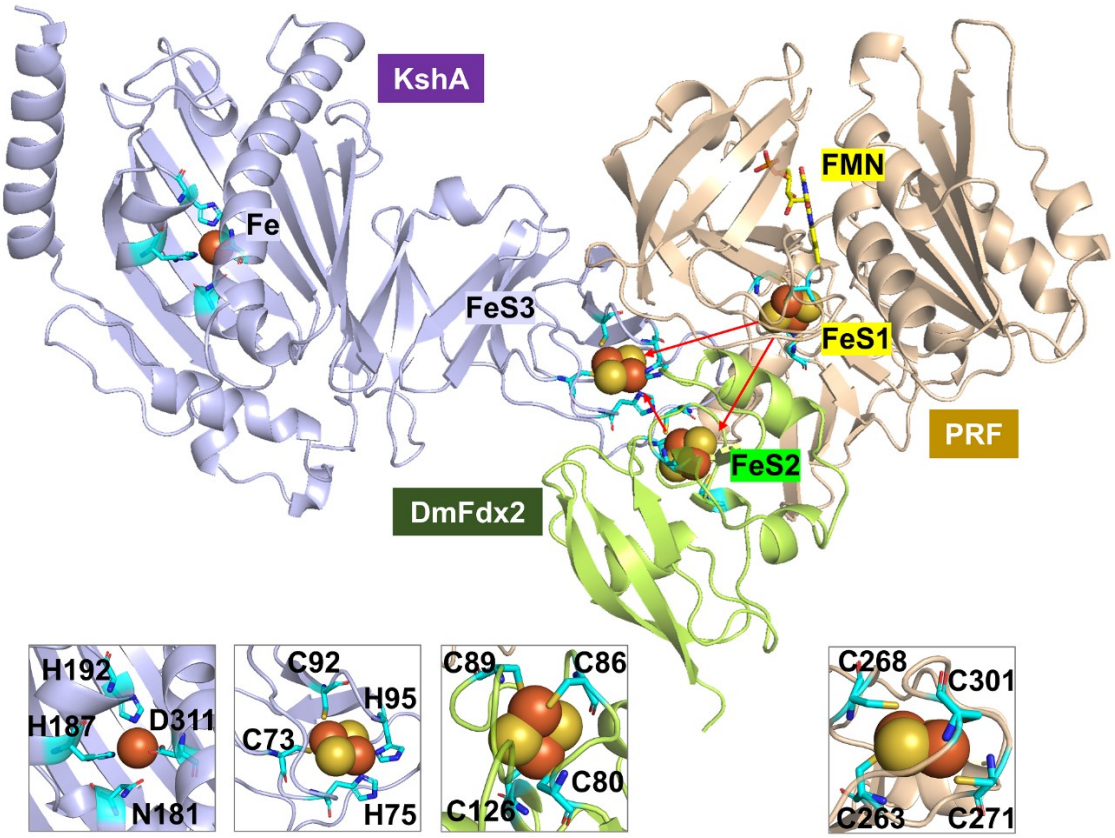

Figure S1. The direct electron transfer (DET) pathways in multienzyme complex. The overall structures of reductase PRF (golden), free ferredoxin DmFdx2 (green) and oxygenase KshA (purple) are shown as cartoon. FMN are shown as sticks. The coordination amino acids of Fe atoms and [2Fe-2S] clusters are shown as sticks.

Figure S2

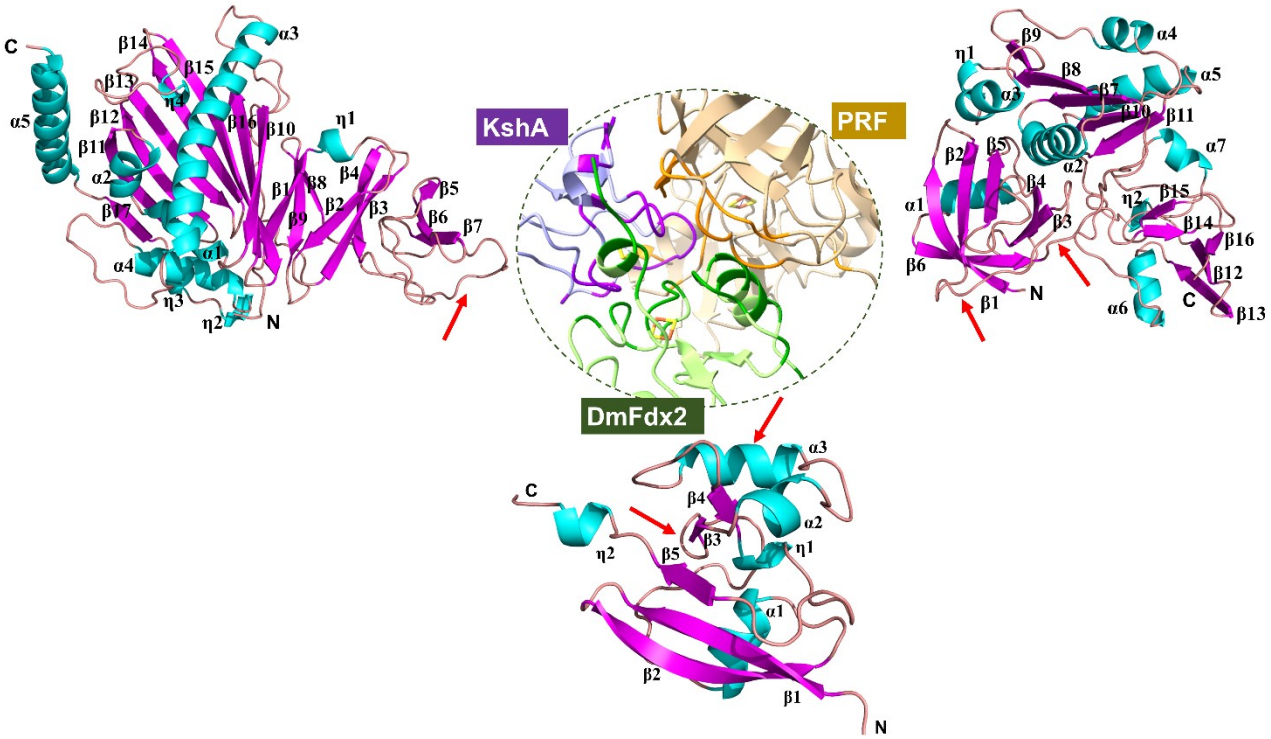

Figure S2. The interface interactions in multienzyme complex. The structures involved in interface interactions are marked by red arrows. The α-helices (cyan) and β-strands (salmon) in structures of reductase PRF, free ferredoxin DmFdx2 and oxygenase KshA are labeled.

Figure S3

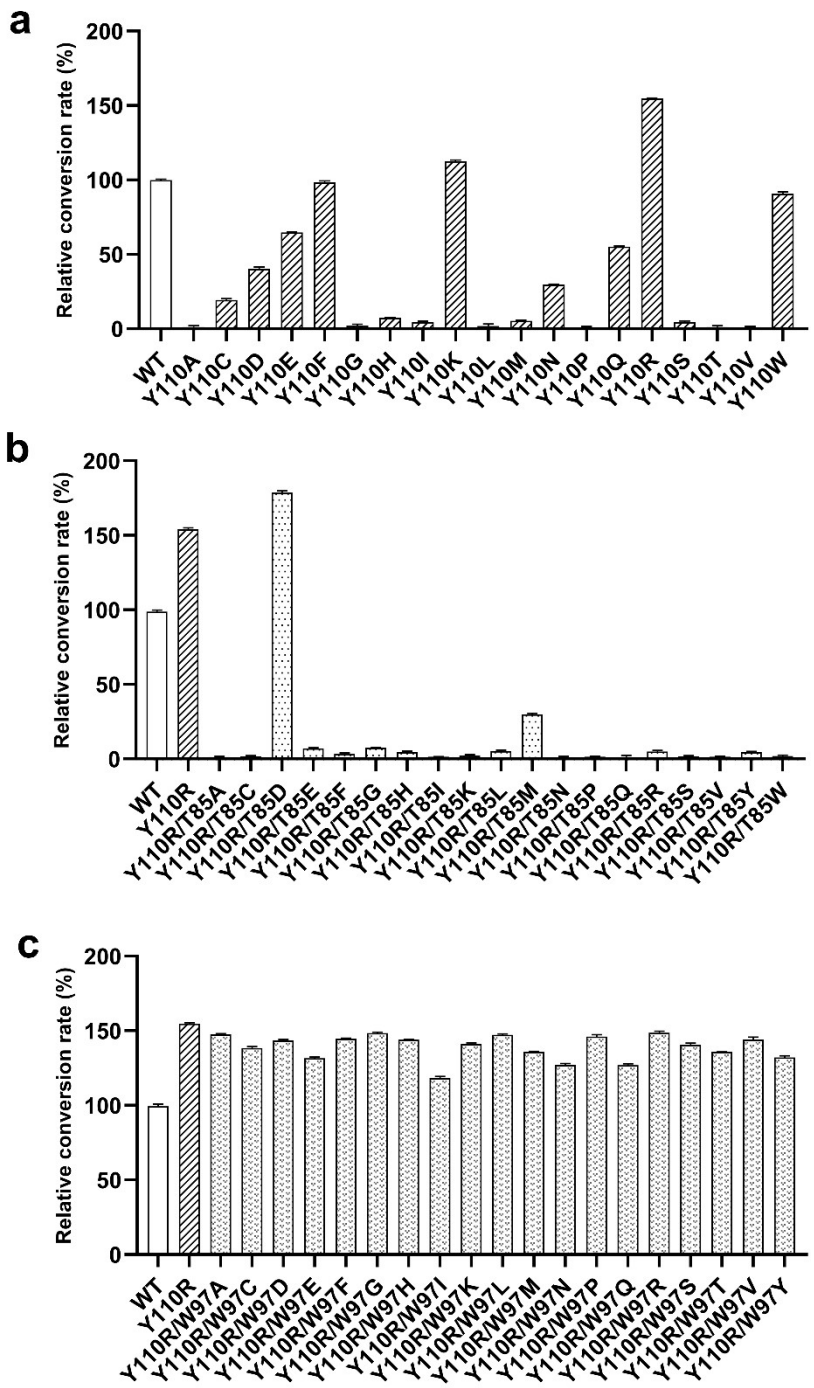

Figure S3. The results of iterative saturation mutagenesis (ISM). (a) The relative conversion rate of Y110 mutants in KshA with WT PRF+DmFdx2. (b) The relative conversion rate of T85 mutants in DmFdx2 with MT1 (Y110R in KshA) + WT PRF. (c) The relative conversion rate of W97 mutants in MT1 with WT PRF+DmFdx2.

Figure S4

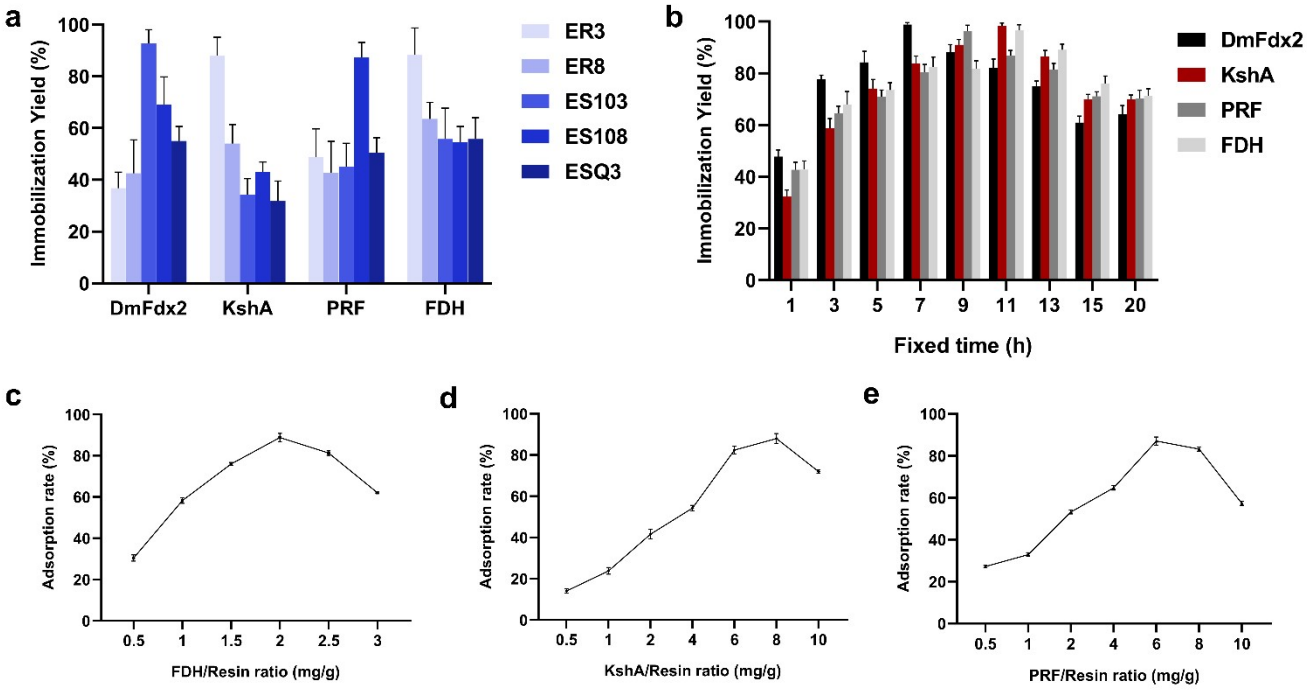

Figure S4. Optimization of immobilization conditions. (a) Optimization of immobilized epoxy resin. (b) Optimization of fixed time on epoxy resin. Optimized immobilization ratio of FDH and epoxy resin (c), KshA and epoxy resin (d), PRF and epoxy resin (e).

Figure S5

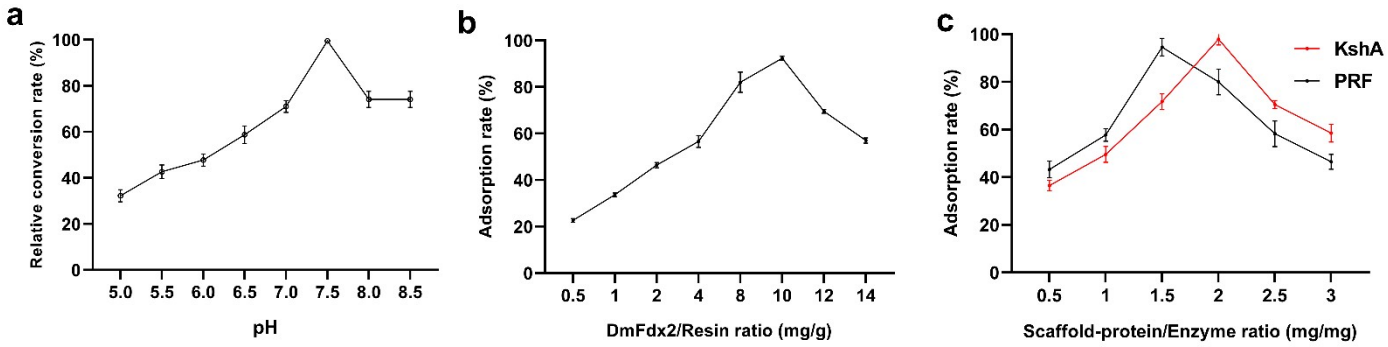

Figure S5. Optimization of scaffold-protein-modified self-assembly directed immobilization. (a) Optimized immobilization pH of ferredoxin DmFdx2. (b) Optimized immobilization ratio of DmFdx2 and epoxy resin. (c) Optimized immobilization ratio of scaffold-protein-modified epoxy resin and KshA, scaffold-protein-modified epoxy resin and PRF.

Figure S6

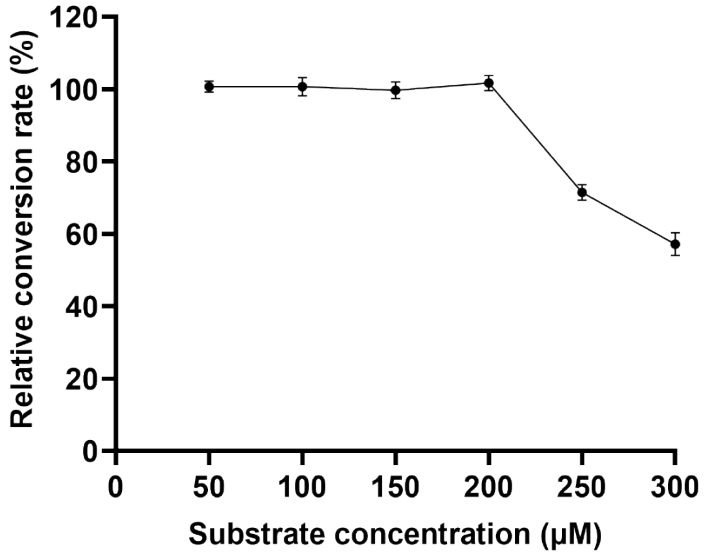

Figure S6. Optimization substrate concentrations of scaffold-protein-modified self-assembly directed immobilization. The immobilized multienzyme catalysis was performed and mixed with 50 mM phosphate buffer (pH 7.5), 500 μM NAD^+, 1.75 mM sodium formate and immobilized proteins (self-assembly immobilized complex at the optimized ratio: 1 mg/mL reductase, 1.5 mg/mL Fdx, 0.75 mg/mL KshA), 0.25 mg/mL immobilized FDH with varying concentrations of AD dissolved in 2% methanol.

Figure S7

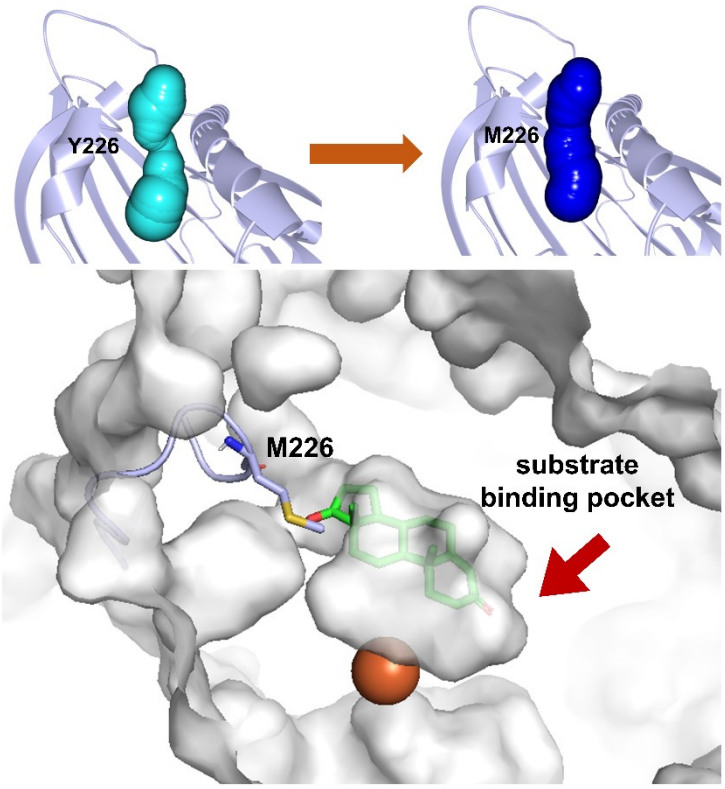

Figure S7 Modification of rate-limiting residues in the substrate channel leading into the binding pocket. Simulation of the substrate channel leading into the binding pocket by CAVER analyst v3.0.363, shown in cyan (WT Y226 in KshA) and blue (mutant M226 in KshA). Oxygenase KshA (gray) is shown as surface. Key residues and the substrate AD (green) are shown as sticks.

Figure S8

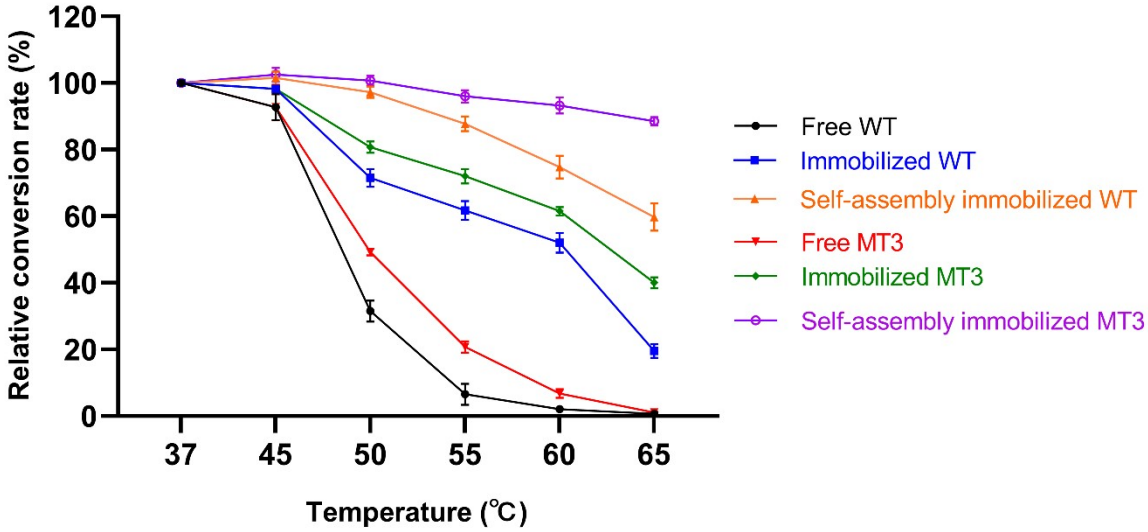

Figure S8. The thermostability of WT complex and mutant complex. The thermostability of free WT complex and MT3(Y110R/Y226M in KshA, T85D in DmFdx2) complex, separately immobilized multienzyme WT complex and MT3 complex, scaffold-protein-modified self-assembly immobilized WT complex and MT3 complex at 37-65 ℃ are shown.